

Exchange Energy in Asymmetric Double Quantum Dots

Emad S. Taiyh¹, Sabah M. M. Ameen¹

¹Physics Department, College of Science, University of Basrah, Iraq

DOI: <https://doi.org/10.5281/zenodo.13304928>

Published Date: 12-August-2024

Abstract: Exchange interaction in Si double quantum dots, which have been suggested as appropriate candidates for spin qubits because of their long spin coherence durations, is investigated here. Using three distinct models of the double quantum dot (DQDs) potential as a function the inter-dot distance (d) and of the electric field (E), inside the Heitler-London (HL) and Hund-Mulliken (HM) approximations, we derive the J-interaction. In a connected double quantum dot (DQD), we evaluate the J-interaction between triplet and singlet states using COMSOL Multiphysics wave functions. Considering several potentials, this computation is carried out inside a specified area of interest. We compare these results with a case in which the 1D Schrödinger problem has precisely known solutions.

Keywords: Double quantum dots; Exchange interaction; Quantum computing.

1. INTRODUCTION

In the last decade, quantum dots have gained significant interest for their potential in scalable quantum computing [1, 2]. Quantum computers process information stored in "quantum bits" (qubits) [3]. With fundamental operations, or "universal quantum logic gates," a quantum computer can solve any problem [4]. Semiconductor quantum dots hosting spin qubits are highly promising due to their long coherence times, high control fidelities, and scalability [5-8]. Qubits can be encoded using the spin states of electrons in various ways, including single-spin, singlet-triplet [9-13], resonant exchange [6, 14], and hybrid spin [15-17]. Many of these systems use tunneling-based effective J-interaction for qubit coupling, allowing for fast, electrically controlled gates [18-20].

By changing the dots from zero onwards, one can attain incremental control over the electron count in GaAs heterostructures [21]. Spin-based quantum computer designs depend critically on the interaction of localized electrons. The first Loss-DiVincenzo (LDV) theory demonstrated that two-qubit gates such as SWAP and controlled-NOT gates could be achieved by means of electrical regulation of J-interaction [22]. Several qubit designs have been suggested, including the single-spin qubit—which is modeled by electron spin states [22, 23]. and the ST0 qubit using $|S\rangle$ and $|T\rangle$ states of two-electron configurations [19]. the exchange-only qubit and the resonant-exchange qubit use particular three-electron states in triple quantum dots. [24, 25].

Thanks to its outstanding spin coherence characteristics, silicon is becoming more and more known as a potential material for spin quantum-information processors [26]. Its natural form can be further purified isotopically and features minimal nuclear spins (5% of Si with a spin of 1/2). A main problem in III-V materials like GaAs, the weak hyperfine interaction in silicon lowers electron-spin decoherence. Furthermore lacking piezoelectric interaction and showing minimal spin-orbit interaction, silicon delays electron spin relaxation by phonons [27-29]. Silicon's conduction band structure with six equivalent minima offers a problem, though. We used the complete configuration interaction computation technique [30] in order to obtain exact findings.

Calculating J-interaction in Silicon (Si) for quantum information processing presents unique challenges compared to Gallium Arsenide (GaAs) [31, 32]. The lower-kappa dielectric in Si strengthens Coulomb interactions, and the larger

effective mass reduces kinetic energy, enhancing correlation effects in Si double quantum dots. This limits the use of simpler J-interaction models successful for GaAs. Additionally, Si's six conduction band minima affect the energy levels and spin structure of electrons in quantum dots, further complicated by confinement and strain which split these valleys into distinct energy levels [33, 34]. These factors create a more complex energy landscape in Si, posing challenges for calculating J-interaction and designing efficient spin-based quantum information devices.[35].

Conveniently derived qubit features, including the J-interaction and energy spectra of the ST0 qubit, using Fock-Darwin (FD) states, configuration interaction method calculations depend on external factors like electric and magnetic field strength and environmental noise[36, 37]. Commonly utilized approximations for investigating the J- interaction in the ST0 qubit are HL and HM ; HM is more accurate [1, 38] . Furthermore, knowledge of energy splitting in Si quantum dot qubits depends on a proper definition of valley-orbit coupling.[36, 39-41] .

This study investigates the effect of environmental electrical fluctuations on spin qubits, crucial for quantum information processing. Finite J-interaction makes these qubits vulnerable to noise from gate electrodes and background charge variations, originating from trapped electrons in the semiconductor material. Movement of these trapped charges can modify barriers between quantum dots, leading to fluctuations in their confining potentials, thereby impacting qubit function.[42, 43].

This paper investigates exchange-gate behavior in double quantum dot (DQD) structures within (Si/SiO₂) [44-46]. Emphasizing characteristics include dot separation, confinement potential, and external electric field. We find wave functions for many DQDs potential profiles, including those under influence of an external electric field, using COMSOL Multiphysics. Using approximation methods such as HL and HM models, J-interaction is then computed evaluating their fit for calculating exchange splitting in Silicon Double Quantum dots. This work offers understanding of exchange gate behavior and various DQD potential models by integrating COMSOL simulations with approximative methods.

This document uses a methodical approach. Section II presents the formalism, including exchanges on their limitations of validity, model potentials for double quantum dots, and methods of determining their coupling connection. Using the HL) and HM approaches, Section III shows computation results with J-interaction as a function of inter-dot distance. Section IV closes the paper at last.

Theoretical Formalism

Consider a Double Quantum Dot (DQD) situated at the silicon (Si) and silicon dioxide (SiO₂) interface, oriented along the z-axis. The Hamiltonian describing the effective mass of two electrons in the DQD is given by [1]:

$$H = \sum_{i=1,2} \hat{h}_i + \frac{e^2}{kr_{12}} = \sum_{i=1,2} \hat{h}_i + \hat{C} , \tag{1}$$

where i=1,2 represent the labels for the two electrons, \hat{h}_i refers to the single-particle Hamiltonian, k is the effective dielectric constant, which takes into account the image charge in the surrounding SiO₂ and is calculated as $k = (\epsilon_{Si} + \epsilon_{SiO_2}) / 2$. r_{12} represents the distance between the two electrons. The Hamiltonian that describes the behavior of a single electron is:

$$\hat{h}_i = \hat{T}_i + V_{ri} + eEx_i + g_{eff\mu_B}BS_{iz} , \tag{2}$$

$$\hat{T}_i = \frac{1}{2m} \left[p_i - \frac{e}{c} A(r_i) \right]^2 . \tag{3}$$

The effective mass in the traverse direction (z and -z direction) is denoted by m and has a value of $0.191m_e$ for Si/SiO₂ DQD. The vector potential $A(r_i)$ represents the magnetic field in the z direction. Specifically, $A(r) = \frac{B}{2}(-y, x, 0)$. However, our discussion will exclude the consideration of the vector potential because it is not applicable to solvable solutions, which are limited to 1D situations. The electric field, represented by E , is oriented in the x-direction to shift the potential well in the z-direction. The term $g_{eff\mu_B}BS_{iz}$ refers to the effective g-factor multiplied by the Bohr magneton. The term " BS_{iz} " denotes the Zeeman energy of the electrons, whereas " $V(r_i)$ " describes the potential confinement experienced by the electrons in the DQDs. In this work, we computed the asymmetric double quantum dots' J-interaction when an external electric field was applied. In this investigation, three distinct potentials were employed: The first is V^Q model [47].

$$V^Q(x) = ax^2 + bx^4 \quad b > 0 \quad (4)$$

while the second is a V^{BQ} model[38].

$$V^{BQ}(x) = \frac{1}{2}m\omega_0^2(\min[(x - d)^2, (x + d)^2]). \quad (5)$$

Note that both of these potentials provide infinite confinement. A third, the exactly solve the double-well model (V^{CA}) [48],

$$V^{CA}(x) = -2 \frac{(a^2 - b^2)[a^2 \cosh^2(bx) + b^2 \sinh^2(ax)]}{[a \cosh(ax) \cosh(bx) - b \sinh(ax) \sinh(bx)]^2} \quad (6)$$

where a and b are the parameters that control the features of the potential well. The well features were controlled by the absolute value of a and b and the relationship between them. For the quartic potential from Eq. (4). The minimum value of the double well case ($a < 0$) is given by $V_{min} = -\frac{a^2}{4b}$ at $x = \pm \sqrt{\frac{|a|}{2b}}$. Determining the distance between the dots. In the bi-quadratic potential (Eq. (5)), the interdot distance is fixed, but the central barrier height $Vb = \frac{1}{2}m\omega_0^2 d^2$, is larger than that of the quartic potential. These potentials exhibit a relationship between barrier height and interdot distance. In experiments, typically, three independent voltages control the DQDs potential, but often only two are varied simultaneously. The model potentials are designed so that around the centers of the dots, the confinement is approximately parabolic, resembling harmonic oscillator states. In the case of the V^{CA} (Eq. (6)), the well features are also controlled by the absolute values of a and b, where $a > b$. This ensures a double-well characteristic with a maximum value of 0 for the energy of a free particle. If $a < b$, the potential shows double barrier characteristics instead. The well separation is determined by the difference between a and b, with a larger difference resulting in closer well separation.

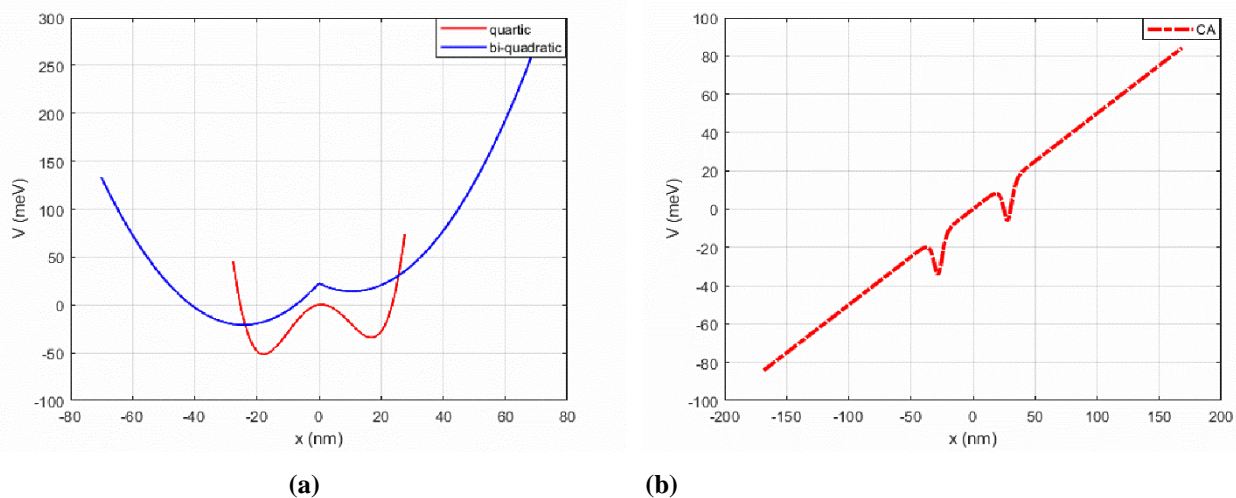


Fig 1: The asymmetric DQD for different potential. (a). The solid red line corresponds to the V^Q , the solid blue line corresponds to the V^{BQ} . (b) V^{CA} .

In Figure 1, for the quartic and V^{CA} , there are minima on both sides of the potential well, with the barrier height between the dots strongly influenced by the electric field. However, for the V^{CA} with an added electric field, the wall moves and gets lower. Commonly employed in research on asymmetric DQDs, the detuning energy λ reflects variations in the DQDs potential along a designated line in the charge stability diagram [49]. The single-particle ground states in the two dots vary in ϵ , thus does as well. Small quantum dots with substantial on-site Coulomb repulsion require a biased and asymmetric DQD, approximated by adding an in-plane electric field ($E=E_x$). Although adding E eliminates the two minima of the potential for all three models, their responses vary greatly. E modulates the potential minima and curvatures of the V^Q , therefore influencing the single-dot confinement energies of the $\psi_{L/R}^{COM}$ states.

Essential physical parameter enabling quantum computing in the ST0 qubit architecture is the energy difference between the unpolarized triplet state $|T_0\rangle$ and the singlet state $|S\rangle$. Energy splitting is the phenomena of J-interaction $= E_{T_0} - E_S$. Four spin eigenstates in a uniform magnetic field will arise if the DQD has two electrons and their interaction is restricted to the Coulomb interaction. With a total spin of $S = 0$, these states are a singlet state $|S\rangle = \frac{1}{\sqrt{2}}(|\uparrow\downarrow\rangle - |\downarrow\uparrow\rangle)$ with a total spin of $S = 0$ and three triplet states $(|T_{0,+,-}\rangle = \frac{1}{2}(|\uparrow\downarrow\rangle + |\downarrow\uparrow\rangle, |\uparrow\uparrow\rangle, |\downarrow\downarrow\rangle)$ with a total spin of $S = 1$. The two techniques HL and HM that can be used to compute the J-interaction will be thoroughly explained in this work.

Heitler-London Approach

Considering only the singly occupied states, $|S(1, 1)\rangle$ and $|T_0(1, 1)\rangle$, and assuming a doubly occupied singlet state, the HL technique offers a direct calculation of the J-interaction. Treating our system as a pair of hydrogen-like artificial atoms, we use the Heitler-London approach, also known as the valence bond approximation, to calculate the J-interaction component. The $|S\rangle$ and $|T\rangle$ states are indicated by [50].

$$|S/T_0\rangle = \frac{|\psi_L(1)\psi_R(2)\rangle \pm \psi_L(1)\psi_R(2)\rangle}{\sqrt{2(1 \pm \ell^2)}} \quad (7)$$

The overlap between the left $|\psi_L\rangle$ and right $|\psi_R\rangle$ dot single electron states is denoted by ℓ and is defined as the inner product of the state $\ell = \langle\psi_L|\psi_R\rangle$. The J-interaction, denoted as the energy difference between $|S\rangle$ and the unpolarized state $|T_0\rangle$, can be expressed as:

$$J_{HL} = \langle T_0|\hat{H}|T_0\rangle - \langle S|\hat{H}|S\rangle \quad (8)$$

which can be rewritten in a simpler form as:

$$J_{HL} = \frac{2\ell^2}{1-\ell^4} (W_v + D_0 - \frac{1}{\ell} E_0) \quad (9)$$

The explicit form of each element in eq. (8) shown as follows:

W_v is the kinetic energy gain of the singlet state.

$$W_v = (u - \frac{w}{\ell}) \quad (10)$$

Where :

$$u = V_{qL}^{LL} + V_{qR}^{RR} = \langle\psi_L|V_q - V_L|\psi_L\rangle + \langle\psi_R|V_q - V_R|\psi_R\rangle \quad (11)$$

$$w = V_{qL}^{RL} + V_{qR}^{LR} = \langle\psi_R|V_q - V_L|\psi_L\rangle + \langle\psi_L|V_q - V_R|\psi_R\rangle \quad (12)$$

$$D_0 = \langle\psi_L(1)\psi_R(2)|\hat{C}|\psi_L(1)\psi_R(2)\rangle \quad (13)$$

$$E_0 = \langle\psi_L(1)\psi_R(2)|\hat{C}|\psi_R(1)\psi_L(2)\rangle \quad (14)$$

D_0 represents the Coulomb interaction contribution, while E_0 represents the exchange Coulomb interaction. It is evident that when the precise solutions and their matching potential functions are utilized in any scenario.

Hund-Mulliken Approach

Let us examine the HM method for molecular orbitals. which extends the HL method by incorporating two doubly occupied spin singlet states. This results in a four-dimensional orbital Hilbert space and includes the states $|S(2, 0)\rangle$ and $|S(0, 2)\rangle$ in the Hamiltonian H , forming a 4×4 matrix. Research shows that the HM technique is more precise in estimating the J-interaction due to its rigorous process [1, 38]. The first step is the orthonormalization of the single-electron wave function using two functions.

$$\phi_L = L(x) \quad (15 a)$$

$$\phi_R = \frac{1}{\sqrt{1-\ell^2}} \langle R(x) - \ell L(x) \rangle \quad (15 b)$$

The DQD features orthonormalized wave functions representing single electron states, including two doubly occupied singlets $|S(2, 0)\rangle$. Additionally, it can generate the (1,1) triplet $|T(1, 1)\rangle$, the (1,1) singlet $|S(1, 1)\rangle$, and $|S(0, 2)\rangle$. The spatial wave functions for these states are expressed as follows:

$$\psi_{L/R}^d(r_1, r_2) = \phi_{\bar{L}}(r_1)\phi_{\bar{L}}(r_2) \quad , \quad (16)$$

$$\psi_{S/T}^{(1,1)}(r_1, r_2) = \frac{1}{\sqrt{2}}[\phi_L(r_1)\phi_R(r_2) \pm \phi_L(r_2)\phi_R(r_1)] \quad . \quad (17)$$

The states that are occupied by two particles are denoted by the superscript. The Hamiltonian expressed in the $S(2, 0)$, $S(0, 2)$, $S(1, 1)$, $T(1, 1)$ basis can be represented as follows

$$H = \begin{bmatrix} 2\varepsilon_L + U & X & W & 0 \\ X & 2\varepsilon_R + U & W & 0 \\ W & W & V_s & 0 \\ 0 & 0 & 0 & V_T \end{bmatrix} \quad , \quad (18)$$

where

$$\varepsilon = \varepsilon_R - \varepsilon_L \quad , \quad (19)$$

$$\varepsilon_R = \langle \phi_R | h_0 | \phi_R \rangle \quad , \quad \varepsilon_L = \langle \phi_L | h_0 | \phi_L \rangle \quad , \quad (20)$$

where h_0 the single particle Hamiltonian.

$$X = \langle \psi_{L/R}^d | \hat{C} | \psi_{R/L}^d \rangle \quad , \quad (21)$$

$$U = \langle \psi_{L/R}^d | \hat{C} | \psi_{L/R}^d \rangle \quad , \quad (22)$$

$$W = \frac{1}{\sqrt{2}} \langle \psi_{L/R}^d | \hat{C} | \psi_s^{(1,1)} \rangle \quad , \quad (23)$$

$$V_s = \left[\varepsilon + \frac{1}{2} \langle \psi_s^{(1,1)} | \hat{C} | \psi_s^{(1,1)} \rangle \right] \quad , \quad (24)$$

$$V_T = \left[\frac{1}{2} \langle \psi_T^{(1,1)} | \hat{C} | \psi_T^{(1,1)} \rangle \right] \quad , \quad (25)$$

The energy of individual particles in the left and right dots in the previous matrix are denoted by ε_L and ε_R , respectively. The different between them in ε which serves as the detuning parameter. U represents the Coulomb repulsion that occurs on-site. V_s and V_T are the Coulomb energies associated with the $|S\rangle$ and $|T\rangle$ states of (1,1) respectively. $\psi_{T/S}^{(1,1)}$ is formed by using orthogonalized single-electron orbitals. X can be likened to an interdot Coulomb exchange integral and a W Coulomb matrix element. All these quantities can be represented in terms of the corresponding matrix elements between the initial, non-orthogonal, left, and right orbitals $\phi_{L/R}$. These matrix elements, referred to as D_0 , E_0 , X , etc., represent the naked orbital interactions.

Extraction of eigenvalues and eigenvectors from the 4×4 Hamiltonian matrix generates the energy diagram for the two-dot system (eq. (18)). Every eigenvector precisely matches an energy value. A mixed state could be a pure basis state or a state vector having probability connected with several bases. By analyzing numerical values for matrix elements under the effect of elements like potential well separation and detuning strength, one computes the energy of every electron state. Subtracting the energy of the $|T\rangle$ states from that of the $|S\rangle$ state allows one to find the J -interaction between singlet state $|S\rangle$.

Using Fock-Darwin states can sometimes provide analytical solutions for both Coulomb and kinetic terms. However, the complexity of the wave functions, as described by Caticha [48], makes analytic solutions unattainable. Therefore, numerical integration methods were employed as an alternative. With COMSOL Multiphysics, we investigated the J -interaction in the ST_0 qubit architecture. This study allowed us to determine the wave functions for both the left ψ_L^{COM} and right ψ_R^{COM} states, facilitating calculations on the J -interaction.

2. RESULTS AND DISCUSSION

We calculate the J-interaction between |S) and |T) states in a linked DQDs near a silicon/silicon dioxide (Si/SiO₂) interface using COMSOL Multiphysics wave functions. The quartic and bi-quadratic potential parameters were adjusted to match the potential function of CA, maintaining consistent dot spacing. Our calculations consider dot sizes achievable in experiments, investigating the impact of confinement energy and inter-dot distance on exchange in asymmetric DQDs for three different potential models. We also examine the impact of inter-dot distance on J-interaction using the HL and HM approaches and discuss the effect of external electric fields on J-interaction.

We calculate the probability amplitudes of the wave functions ψ_L^{COM} , ψ_R^{COM} from the numerical solution of the Schrödinger equation for three DQDs potential models. For the V^Q model, $a = -2$ and $b = 0.5$ [47], for the V^{BQ} model, $a = 2.2361 \times 10^8$; and for the V^{CA} model, $a = 2.2361 \times 10^8$ and $b = 2.2305 \times 10^8$. [51]. To determine the J-interaction, we first calculate the wave functions for the left and right dots using a splitting potential for asymmetric DQDs, as shown in Figures 2, 3, and 4.

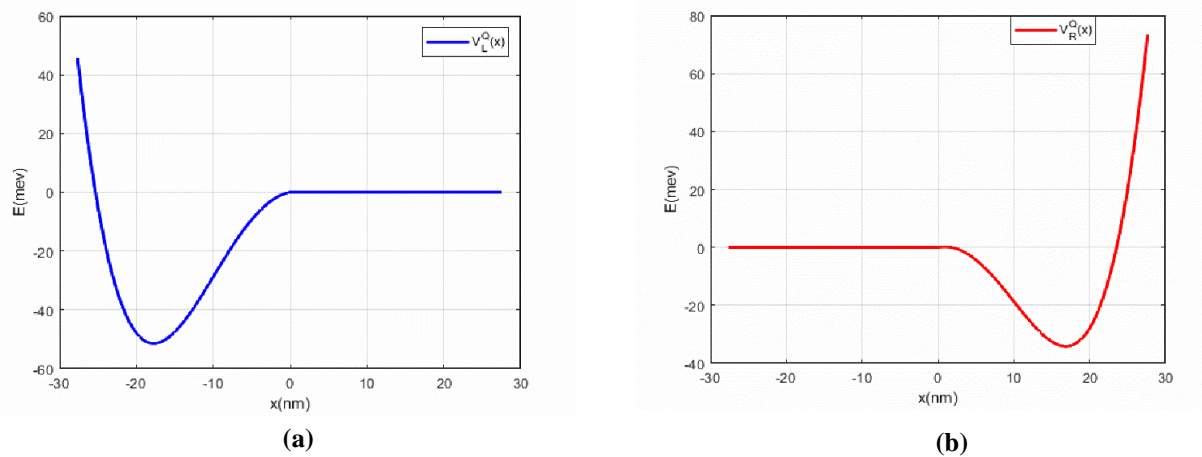


Fig 2: Quartic potential splitting (a) the solid blue line corresponds to the Left V_L^Q (b) the solid red line corresponds to the Right V_R^Q .

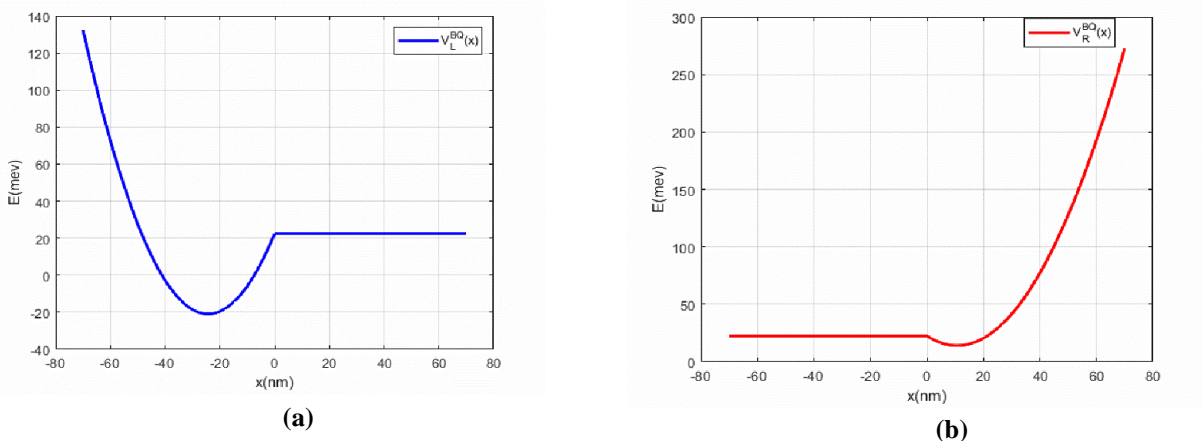


Fig 3: Bi-quadratic potential splitting (a) the solid blue line corresponds to the Left V_L^{BQ} . (b) the solid red line corresponds to the Right V_R^{BQ} .

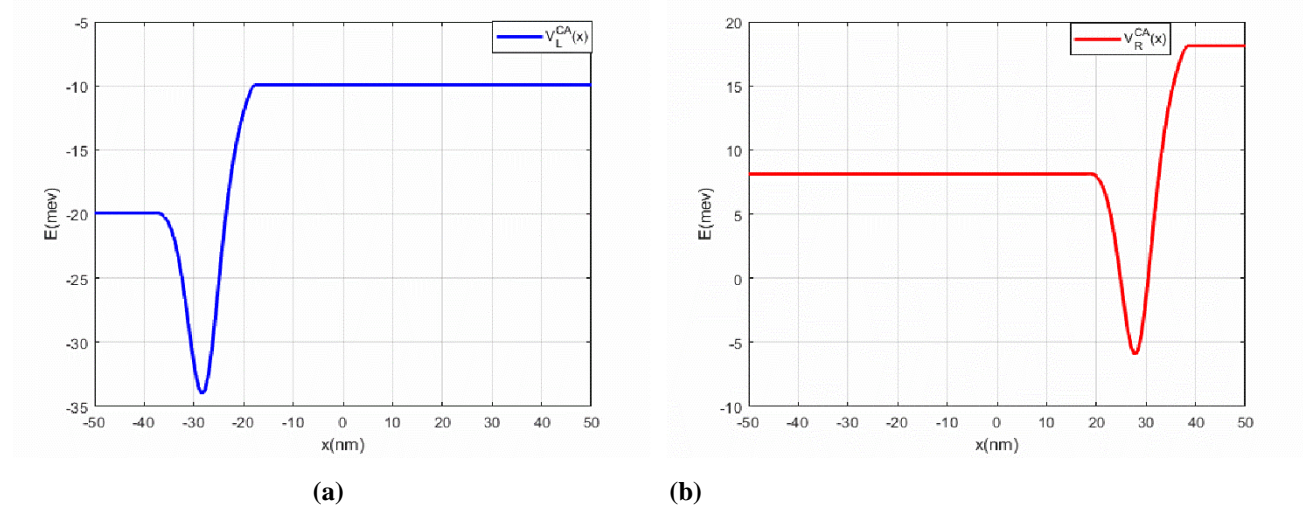


Fig 4: Caticha (CA) potential splitting (a) the solid blue line corresponds to the Left V_L^{CA} (b) the solid red line corresponds to the Right V_R^{CA}

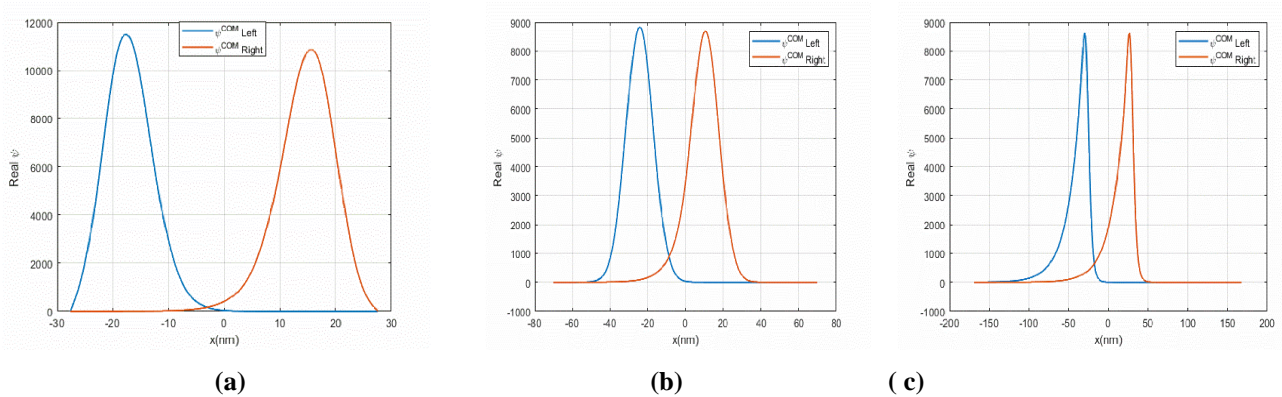


Fig 5: COMSOL wave functions ψ_L^{COM} , ψ_R^{COM} corresponding to V^Q (a), V^{BQ} (b), and V^{CA} (c)

J-interaction as a function of interdot distance

In this section, we determine the J-interaction as a function of inter-dot distance (d) while keeping the well depth constant. The well depth and potential barrier are chosen to match those of the quartic and bi-quadratic potentials used for FD states ($\hbar\omega_0 = 7.658$ meV). Figures 6, 7 and, 8 show that the J-interaction increases with the applied electric field due to changes in the electrons' potential energy landscape and distribution within each dot. The electric field can enhance coupling by increasing the overlap of electron wavefunctions or, in some cases, weakening it by pushing electron distributions apart.

At certain inter-dot distances, the J-interaction changes with increasing E, causing J's dependence on d to become nonmonotonic. Remarkably, J behaves similarly as a function of d across different potential models. This result is explained by the overlap between the wave functions of the left and right dots (ψ_L, ψ_R). Increased spacing reduces overlap, decreasing Coulomb interaction and inter-dot hopping, ultimately weakening the J-interaction.

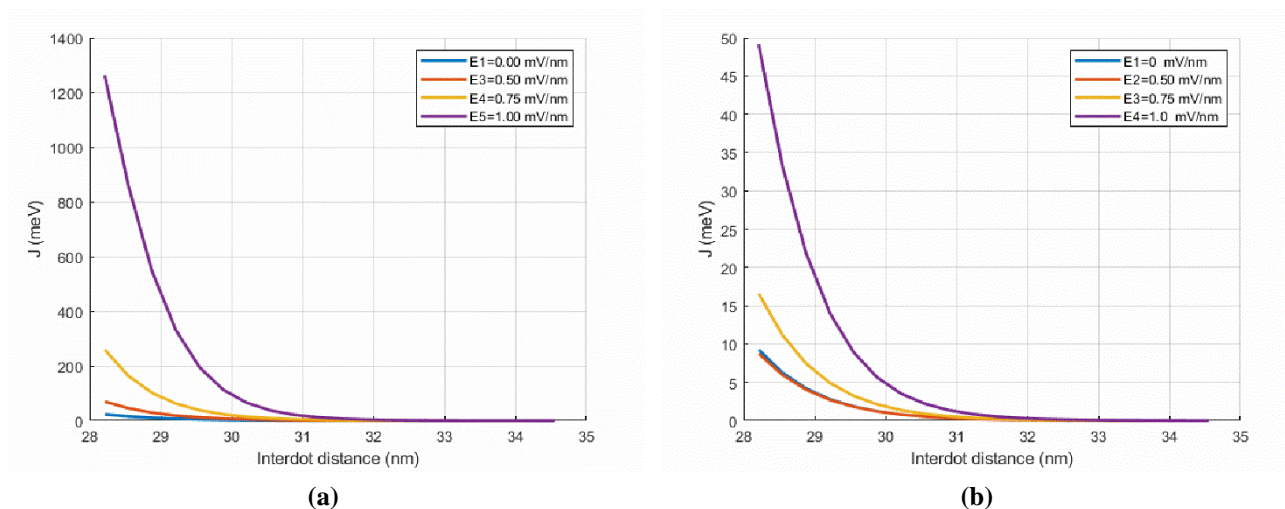


Fig6: Calculated exchange interaction vs. inter-dot distance for V^Q (a) HL approach (b) HM approach

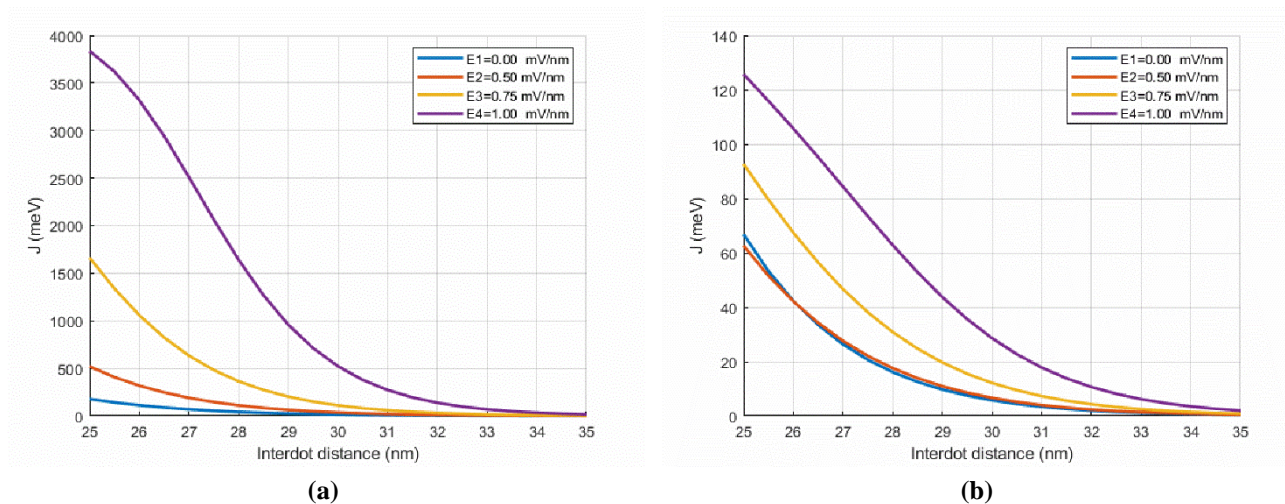


Fig7: Calculated exchange interaction vs. inter-dot distance for $1V^{BQ}$ (a) HL approach (b) HM approach

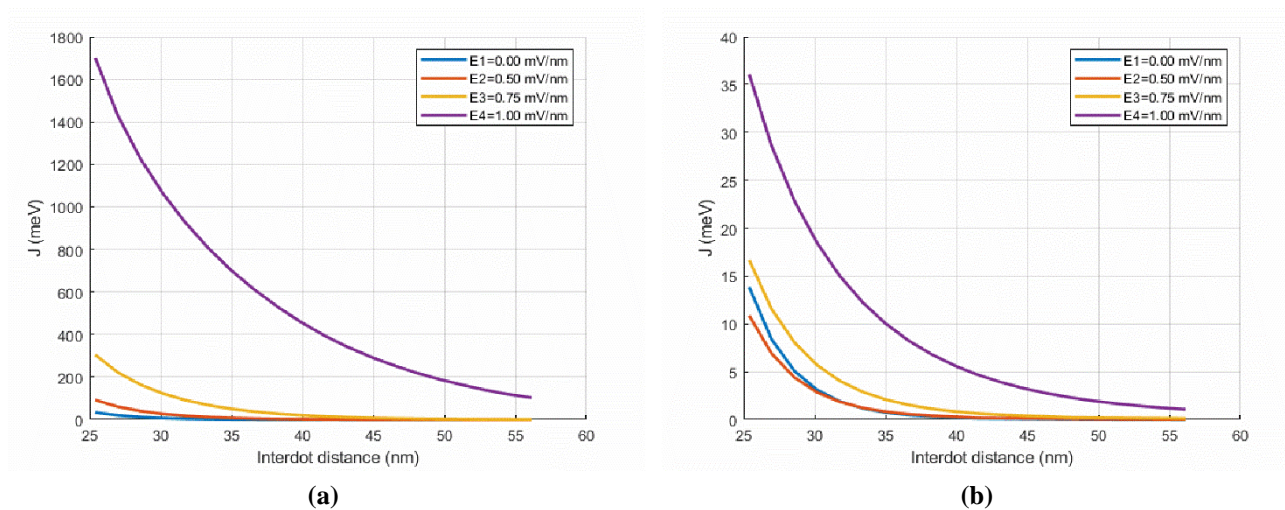


Fig8: Calculated exchange interaction vs. inter-dot distance V^{CA} (a) HL approach (b) HM approach

The HL approach only considers the $|S(1, 1)\rangle$ and $|T_0\rangle$ states, omitting the $|S(2, 0)\rangle$ and $|S(0, 2)\rangle$ states, which may introduce errors in calculating the J-interaction. The HM technique, which includes these states, yields more accurate results. Figure 6 shows that the HL approach predicts a higher J-interaction than the HM approach, aligning with previous studies where HL predictions were at least five times greater. Using COMSOL Multiphysics wave functions, the HM method's inclusion of doubly occupied states significantly impacts the J-interaction accuracy.

When comparing three potentials (quartic, bi-quadratic, and Caticha's CA), the inter-dot distance is plotted against energy exchange (J). Differences in peak values, locations, or shapes among the curves are evident. The choice of potential balances computational efficiency and accuracy: Caticha's CA potential offers the most realistic modeling but requires complex computations, the quartic potential is simplest but less precise, and the bi-quadratic potential offers a balanced approach.

J-interaction as a function of Electric field

The J-interaction was calculated as a function of the electric field (E) while keeping the inter-dot distance (d) constant. Figures 9, 10 and, 11 show that increasing the electric field increases the J-interaction. This is because the electric field lowers the potential barrier between the dots, facilitating electron tunneling and enhancing energy exchange. Additionally, the distance between the quantum dots is crucial; closer dots exhibit stronger energy exchange due to stronger coupling. This demonstrates that even small changes in the electric field, especially at higher strengths, can significantly impact J-interaction.

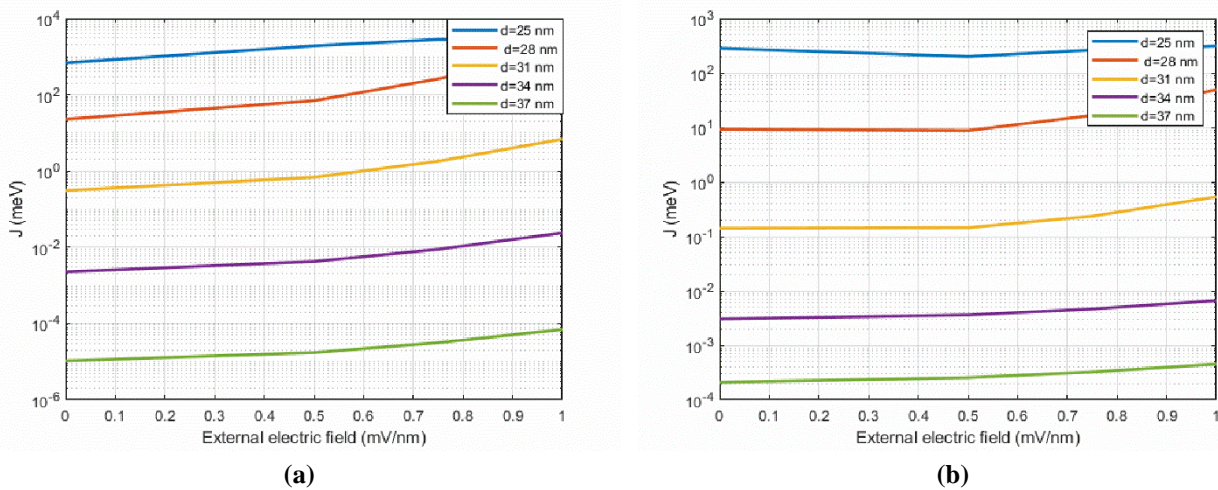


Fig 9: Calculated exchange interaction vs. electric field for V^Q (a) HL approach (b) HM approach.

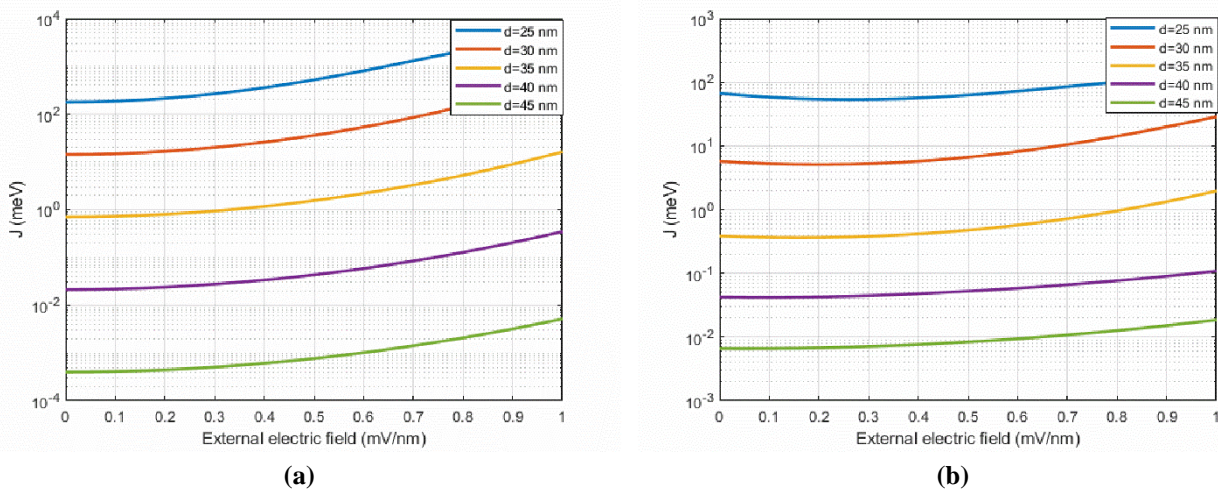


Fig 10: Calculated exchange interaction vs. electric field for V^{BQ} (a) HL approach (b) HM approach.

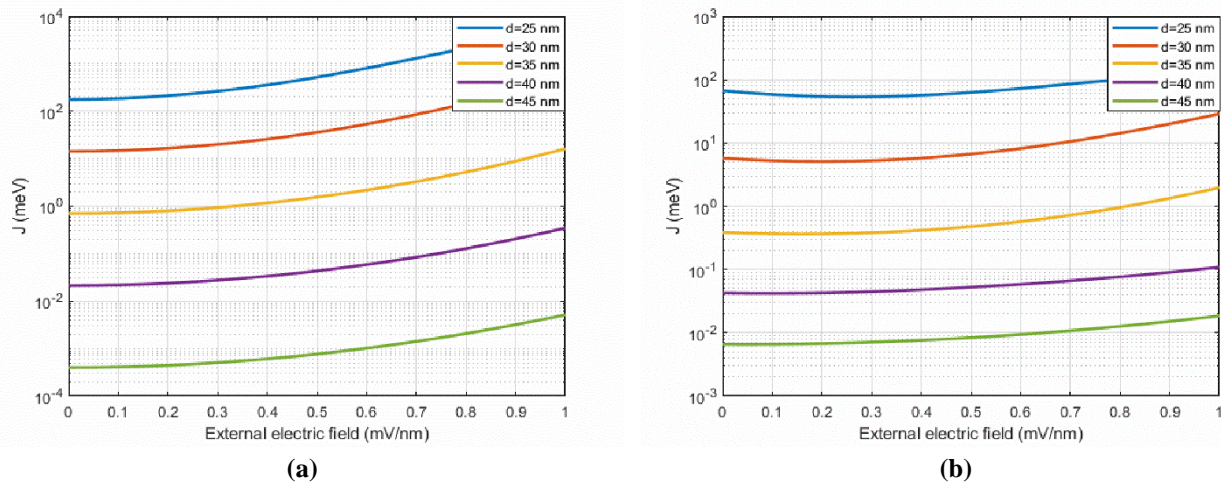


Fig 11: Calculated exchange interaction vs. electric field V^{CA} (a) HL approach (b) HM approach.

3. CONCLUSIONS

The J-interaction is derived from Coulombic interactions between electrons in a system. We computed the J-interaction between two electrons in DQDs formations within a Si/SiO₂ heterostructure using the HL and HM approximations. Wave functions generated by COMSOL Multiphysics were utilized to calculate J-interaction for the |S⟩ and |T⟩ states qubit ST₀, considering various potentials such as V^{BQ} , V^Q , and V^{CA} potentials.

The J-interaction from COMSOL states intriguing characteristics compared to conventional methods. These include a large J due to high interdot probability density and a non-monotonic J curve. An applied electric field increases quantum dot J-interaction, and the exchange behavior varies based on potential fluctuations affecting the interdot distance d. Significant disparities are observed when comparing results from conventional methods using finite difference (FD) states with V^{BQ} , V^Q , and V^{CA} potentials.

REFERENCES

- [1] G. Burkard, D. Loss, and D. P. DiVincenzo, "Coupled quantum dots as quantum gates," *Physical Review B*, vol. 59, no. 3, p. 2070, 1999. <https://doi.org/10.1103/PhysRevB.59.2070>
- [2] M. S. Sherwin, A. Imamoglu, and T. Montroy, "Quantum computation with quantum dots and terahertz cavity quantum electrodynamics," *Physical Review A*, vol. 60, no. 5, p. 3508, 1999. <https://doi.org/10.1103/PhysRevA.60.3508>
- [3] A. J. R. o. P. i. P. Steane, "Quantum computing," vol. 61, no. 2, p. 117, 1998. <https://doi.org/10.1038/20127>
- [4] D. J. P. o. t. R. S. o. L. A. M. Deutsch and P. Sciences, "Quantum theory, the Church–Turing principle and the universal quantum computer," vol. 400, no. 1818, pp. 97-117, 1985. <https://doi.org/10.1098/rspa.1985.0070>
- [5] F. Koppens, K. Nowack, and L. Vandersypen, "Spin echo of a single electron spin in a quantum dot," *Physical Review Letters*, vol. 100, no. 23, p. 236802, 2008. <https://doi.org/10.1103/PhysRevLett.100.236802>
- [6] J. Medford *et al.*, "Quantum-dot-based resonant exchange qubit," *Physical review letters*, vol. 111, no. 5, p. 050501, 2013. <https://doi.org/10.1103/PhysRevLett.111.050501>
- [7] Z. Qi *et al.*, "Effects of charge noise on a pulse-gated singlet-triplet S– T– qubit," *Physical Review B*, vol. 96, no. 11, p. 115305, 2017. <https://doi.org/10.1103/PhysRevB.96.115305>
- [8] J. Taylor *et al.*, "Fault-tolerant architecture for quantum computation using electrically controlled semiconductor spins," *Nature Physics*, vol. 1, no. 3, pp. 177-183, 2005. <https://doi.org/10.1038/nphys174>.

International Journal of Novel Research in Physics Chemistry & Mathematics

 Vol. 11, Issue 2, pp: (59-71), Month: May - August 2024, Available at: www.noveltyjournals.com

- [9] M. Veldhorst *et al.*, "An addressable quantum dot qubit with fault-tolerant control-fidelity," *Nature Nanotechnology*, vol. 9, no. 12, pp. 981-985, 2014/12/01 2014. <https://doi.org/10.1038/nnano.2014.216>
- [10] K. Takeda *et al.*, "A fault-tolerant addressable spin qubit in a natural silicon quantum dot," vol. 2, no. 8, p. e1600694, 2016. <https://doi.org/10.1126/sciadv.1600694>
- [11] D. M. Zajac *et al.*, "Resonantly driven CNOT gate for electron spins," vol. 359, no. 6374, pp. 439-442, 2018. <https://doi.org/10.1126/science.aao5965>
- [12] P. Cerfontaine, T. Botzem, D. P. DiVincenzo, and H. J. P. r. l. Bluhm, "High-fidelity single-qubit gates for two-electron spin qubits in GaAs," vol. 113, no. 15, p. 150.2014 ,501 <https://doi.org/10.1103/PhysRevLett.113.150501>
- [13] X. Wu *et al.*, "Two-axis control of a singlet–triplet qubit with an integrated micromagnet," vol. 111, no. 33, pp. 11938-11942, 2014. <https://doi.org/10.1073/pnas.1412230111>
- [14] E. A. Laird, J. M. Taylor, D. P. DiVincenzo, C. M. Marcus, M. P. Hanson, and A. C. Gossard, "Coherent spin manipulation in an exchange-only qubit," *Physical Review B*, vol. 82, no. 7, p. 075403, 2010. <https://doi.org/10.1103/PhysRevB.82.075403>
- [15] Z. Shi *et al.*, "Fast hybrid silicon double-quantum-dot qubit," *Physical review letters*, vol. 108, no. 14, p. 140503, 2012. <https://doi.org/10.1103/PhysRevLett.108.140503>
- [16] T. S. Koh, J. K. Gamble ,M. Friesen, M. Eriksson, and S. J. P. r. l. Coppersmith, "Pulse-gated quantum-dot hybrid qubit," vol. 109, no. 25, p. 250503, 2012. <https://doi.org/10.1103/PhysRevLett.109.250503>
- [17] G. Cao *et al.*, "Tunable hybrid qubit in a GaAs double quantum dot," *Physical review letters*, vol. 116, no. 8, p. 086.2016 ,801 <https://doi.org/10.1103/PhysRevLett.116.086801>
- [18] B. M. Maune *et al.*, "Coherent singlet-triplet oscillations in a silicon-based double quantum dot," *Nature*, vol. 481, no. 7381, pp. 344-347, 2012. <https://doi.org/10.1038/nature10707>
- [19] J. R. Petta *et al.*, "Coherent manipulation of coupled electron spins in semiconductor quantum dots," *Science*, vol. 309, no. 5744, pp. 2180-4, Sep 30 2005. <https://doi.org/10.1126/science.1116955>
- [20] R. Brunner *et al.*, "Two-qubit gate of combined single-spin rotation and interdot spin exchange in a double quantum dot," vol. 107, no. 14, p. 146801, 2011. <https://doi.org/10.1103/PhysRevLett.107.146801>
- [21] S. Tarucha, D. Austing ,T. Honda, R. Van der Hage, and L. P. Kouwenhoven, "Shell filling and spin effects in a few electron quantum dot," *Physical Review Letters*, vol. 77, no. 17, p. 3613, 1996<https://doi.org/10.1103/PhysRevLett.77.3613>.
- [22] D. Loss and D. P. DiVincenzo, "Quantum computation with quantum dots," *Physical Review A*, vol. 57, no. 1, p. 120, 1998. <https://doi.org/10.1103/PhysRevA.57.120>
- [23] J. T. Muhonen *et al.*, "Storing quantum information for 30 seconds in a nanoelectronic device," *Nature nanotechnology*, vol. 9, no. 12, pp. 986-991, 2014. <https://doi.org/10.1038/nnano.2014.211>
- [24] D. P. DiVincenzo, D. Bacon, J. Kempe, G. Burkard ,and K. B. Whaley, "Universal quantum computation with the exchange interaction," *nature*, vol. 408, no. 6810, pp. 339-342, 2000. <https://doi.org/10.1038/35042541>
- [25] D. Kim *et al.*, "Quantum control and process tomography of a semiconductor quantum dot hybrid qubit," *Nature*, vol. 511, no ,7507 .pp. 70-74, 2014. <https://doi.org/10.1038/nature13407>
- [26] A. Tyryshkin *et al.*, "Coherence of spin qubits in silicon," *Journal of Physics: Condensed Matter*, vol. 18, no. 21, p. S783, 2006. <https://iopscience.iop.org/article/10.1088/0953-8984/18/21/S06/meta>
- [27] P. Harvey-Collard *et al.*, "Spin-orbit interactions for singlet-triplet qubits in silicon ",*Physical review letters*, vol. 122, no. 21, p. 217702, 2019. <https://doi.org/10.1103/PhysRevLett.122.217702>

International Journal of Novel Research in Physics Chemistry & Mathematics

 Vol. 11, Issue 2, pp: (59-71), Month: May - August 2024, Available at: www.noveltyjournals.com

- [28] A. Khaetskii, D. Loss, and L. Glazman, "Electron spin evolution induced by interaction with nuclei in a quantum dot," *Physical Review B*, vol. 67, no. 19, p. 195329, 2003. <https://doi.org/10.1103/PhysRevB.67.195329>
- [29] C. Tahan and R. Joynt, "Rashba spin-orbit coupling and spin relaxation in silicon quantum wells," *Physical Review B*, vol. 71, no. 7, p. 075315, 2005. <https://doi.org/10.1103/PhysRevB.71.075315>
- [30] M. Prada, R. Blick, and R. Joynt, "Singlet-triplet relaxation in two-electron silicon quantum dots," *Physical Review B*, vol. 77, no. 11, p. 115438, 2008. <https://doi.org/10.1103/PhysRevB.77.115438>
- [31] V. Scarola and S. D. J. P. R. A. Sarma, "Exchange gate in solid-state spin-quantum computation: The applicability of the Heisenberg model," vol. 71, no. 3, p. 032340, 2005. <https://doi.org/10.1103/PhysRevA.71.032340>
- [32] J. Pedersen, C. Flindt, N. A. Mortensen, and A.-P. J. P. R. B. Jauho, "Failure of standard approximations of the exchange coupling in nanostructures," vol. 76, no. 12, p. 125323, 2007. <https://doi.org/10.1103/PhysRevB.76.125323>
- [33] T. Ando, A. B. Fowler, and F. J. R. o. M. P. Stern, "Electronic properties of two-dimensional systems," vol. 54, no. 2, p. 437, 1982. <https://doi.org/10.1103/RevModPhys.54.437>
- [34] A. Saraiva, M. Calderón, X. Hu, S. D. Sarma, and B. J. P. R. B. Koiller, "Physical mechanisms of interface-mediated intervalley coupling in Si," vol. 80, no. 8, p. 081305, 2009. <https://doi.org/10.1103/PhysRevB.80.081305>
- [35] D. Culcer, Ł. Cywiński, Q. Li, X. Hu, and S. D. J. P. R. B. Sarma, "Realizing singlet-triplet qubits in multivalley Si quantum dots," vol. 80, no. 20, p. 205302, 2009. <https://doi.org/10.1103/PhysRevB.80.205302>
- [36] E. Nielsen, R. W. Young, R. P. Muller, and M. J. P. R. B. Carroll, "Implications of simultaneous requirements for low-noise exchange gates in double quantum dots," vol. 82, no. 7, p. 075319, 2010. <https://doi.org/10.1103/PhysRevB.82.075319>
- [37] M. A. Bakker, S. Mehl, T. Hiltunen, A. Harju, and D. P. J. P. R. B. DiVincenzo, "Validity of the single-particle description and charge noise resilience for multielectron quantum dots," vol. 91, no. 15, p. 155425, 2015. <https://doi.org/10.1103/PhysRevB.91.155425>
- [38] Q. Li, Ł. Cywiński, D. Culcer, X. Hu, and S. Das Sarma, "Exchange coupling in silicon quantum dots: Theoretical considerations for quantum computation," *Physical Review B*, vol. 81, no. 8, 2010. <https://doi.org/10.1103/PhysRevB.81.085313>
- [39] E. Nielsen, R. P. Muller, and M. S. J. P. R. B. Carroll, "Configuration interaction calculations of the controlled phase gate in double quantum dot qubits," vol. 85, no. 3, p. 035319, 2012. <https://doi.org/10.1103/PhysRevB.85.035319>
- [40] D. Culcer and N. M. J. A. P. L. Zimmerman, "Dephasing of Si singlet-triplet qubits due to charge and spin defects," vol. 102, no. 23, 2013. <https://doi.org/10.1063/1.4810911>
- [41] N. M. Zimmerman, P. Huang, and D. J. N. I. Culcer, "Valley phase and voltage control of coherent manipulation in si quantum dots," vol. 17, no. 7, pp. 4461-4465, 2017. <https://doi.org/10.1021/acs.nanolett.7b01677>
- [42] D. Vion *et al.*, "Manipulating the quantum state of an electrical circuit," vol. 296, no. 5569, pp. 886-889, 2002. <https://doi.org/10.1126/science.1069372>
- [43] G. Ramon and X. J. P. R. B. Hu, "Decoherence of spin qubits due to a nearby charge fluctuator in gate-defined double dots," vol. 81, no. 4, p. 045304, 2010. <https://doi.org/10.1103/PhysRevB.81.045304>
- [44] H. Liu *et al.*, "Pauli-spin-blockade transport through a silicon double quantum dot," *Physical Review B*, vol. 77, no. 7, p. 073310, 2008. <https://doi.org/10.1103/PhysRevB.77.073310>
- [45] H. Liu, T. Fujisawa, H. Inokawa, Y. Ono, A. Fujiwara, and Y. Hirayama, "A gate-defined silicon quantum dot molecule," *Applied Physics Letters*, vol. 92, no. 22, 2008. <https://doi.org/10.1063/1.2938693>
- [46] E. Nordberg *et al.*, "Enhancement-mode double-top-gated metal-oxide-semiconductor nanostructures with tunable lateral geometry," *Physical Review B*, vol. 80, no. 11, p. 115331, 2009. <https://doi.org/10.1103/PhysRevB.80.115331>

International Journal of Novel Research in Physics Chemistry & MathematicsVol. 11, Issue 2, pp: (59-71), Month: May - August 2024, Available at: www.noveltyjournals.com

- [47] Q. Dong, G.-H. Sun, M. A. Aoki, C.-Y. Chen, and S.-H. J. M. P. L. A. Dong, "Exact solutions of a quartic potential," vol. 34, no. 26, p. 1950208, 2019. <https://doi.org/10.1142/S0217732319502080>
- [48] A. Caticha, "Construction of exactly soluble double-well potentials," *Physical Review A*, vol. 51, no. 5, p. 4264, 1995. <https://doi.org/10.1103/PhysRevA.51.4264>
- [49] R. Hanson, L. P. Kouwenhoven, J. R. Petta, S. Tarucha, and L. M. Vandersypen, "Spins in few-electron quantum dots," *Reviews of modern physics*, vol. 79, no. 4, p. 1217, 2007. . <https://doi.org/10.1103/RevModPhys.79.1217>
- [50] W. Heitler and F. London" ,Wechselwirkung neutraler Atome und homöopolare Bindung nach der Quantenmechanik," *Zeitschrift für Physik*, vol. 44, no. 6-7, pp. 455-472, 1927. <https://doi.org/10.1007/BF01397394>
- [51] G. Chan and X. Wang, "On the validity of microscopic calculations of double-quantum-dot spin qubits based on Fock-Darwin states," *Science China Physics, Mechanics & Astronomy*, vol. 61, no. 4, 2018. <https://doi.org/10.1007/s11433-017-9145-6>